Interfacial Phenomena and Heat Transfer, 5(1):59–79 (2017)

STATIONARY STABILITY OF TWO LIQUID LAYERS COATING BOTH SIDES OF A THICK WALL UNDER THE SMALL BIOT NUMBERS APPROXIMATION

L.A. Dávalos-Orozco

Instituto de Investigaciones en Materiales, Departamento de Polímeros, Universidad Nacional Autónoma de México, Ciudad Universitaria Circuito Exterior S/N, Delegación Coyoacán, 04510 México D.F., México; Tel.: +52 55 5622 4601; Fax: +52 55 5616 1201, E-mail: ldavalos@unam.mx

Original Manuscript Submitted: 11/3/2017; Final Draft Received: 11/15/2017

In this paper the linear stability of two liquid layers with flat free-surface coating of both sides of a wall of finite thickness and thermal conductivity is investigated under the assumption that the liquid/gas Biot numbers are very small. It is supposed that gravity is negligible and that the atmospheres at both sides of the system have different temperatures. These conditions allow for the formation of very large thermocapillary convection cells. Thus, the small wave-number approximation is done up to fourth order to calculate the marginal Marangoni number. From this result, the critical Marangoni number (Ma_c) and its corresponding wave number (k_c) have been calculated numerically. The wave number corresponding to the maximum growth rate ($k_{\max}$) is also calculated for a Marangoni number slightly above criticality. It is shown that, under these conditions, the flow is stationary. It is found that Ma_c may have two magnitudes, one positive and another one negative, depending on the magnitude of some particular parameters of the problem. It is shown that k_c may be zero or different from zero with small but finite magnitude. Some parameters are fixed and the numerical results are presented by means of plots of Ma_c, k_c, and $k_{\max}$ against different important parameters of the problem.

KEY WORDS: *thin liquid film, thermocapillarity, marangoni convection, solid interlayer, small Biot number, small wave-number approximation*

1. INTRODUCTION

Thin films on substrates with different thermal properties have been investigated for many years. The thermocapillary problem where the free surface is flat was first investigated by Pearson (1958). In that paper is shown the variation of the critical Marangoni number and corresponding wave number with respect to the Biot numbers of the fluid-wall interface and the fluid-atmosphere interface. The latter is called a free surface because the dynamics of the atmosphere is neglected in comparison to that of the fluid. In the thermal Marangoni problem the condition of a flat free surface was first relaxed by Scriven and Sternling (1964) assuming it is able to deform. When the temperature gradient is such that the wall temperature is larger than that of the atmosphere the liquid film is susceptible of instability after reaching a critical magnitude of the temperature gradient. However, it is shown that when the wall is colder than the atmosphere (heated from above) the film is always stable. In the presence of gravity natural convection phenomena can be neglected if the liquid layer is very thin. However, gravity has a stabilizing effect when the surface is deformable, as shown by Takashima (1981a,b), in the stationary and time-dependent cases, respectively. The problem of double diffusive Marangoni convection was investigated for a flat free surface by McTaggart (1983). Viscoelasticity was included by Getachew and Rosenblat (1985) for a flat surface. Temperature variation of viscosity is taken into account by Slavtchev and Ouzounov (1994) and Kalitzova-Kurteva et al. (1996) for stationary convection with deformable free surface and by Slavtchev et al. (1998) for oscillatory convection and deformable free surface. Due to practical applications, the convenient control of Marangoni convection has been stressed by Bau (1999), Or et al. (1999), and

NOMENCLATURE

bi	fluid 2 scaled Biot number
bi_1	fluid 1 scaled Biot number
Bi	fluid 2 free surface-atmosphere Biot number
Bi_1	fluid 1 free surface-atmosphere Biot number
c_{P1}	fluid 1 heat capacity
c_{P2}	fluid 2 heat capacity
c_{PW}	wall heat capacity
d	fluid 1 over fluid 2 thicknesses ratio
d_2	thickness of fluid 2
d_W	wall over fluid 2 thicknesses ratio
D	d/dz
H_{h1}	fluid 1 coefficient of heat transfer across the free surfaces
H_{h2}	fluid 2 coefficient of heat transfer across the free surfaces
k	magnitude of the wave-number vector
k_C	critical wave number
$k_{\max}$	wave number of the maximum growth rate
k_S	scaled magnitude of the wave number
k_x	x component of the wave number vector
k_y	y component of the wave number vector
K_1	fluid 1 thermal conductivities
K_2	fluid 2 thermal conductivities
K	fluid 1 over fluid 2 thermal conductivities ratio
Ma	fluid 2 Marangoni number
Ma_C	critical Marangoni number
Ma_{1S}, Ma_{2S}	scaled Ma's at different orders
Pr	fluid 2 Prandtl number
T	fluid 2 main temperature profile
T_1	fluid 1 main temperature profile
T_W	wall main temperature profile
$\overline{T}$	fluid 2 dimensionless temperature
$\underline{T_1}$	fluid 1 dimensionless temperature
$\underline{T}$	fluid 2 temperature
$\overline{T_1}$	fluid 1 temperature
T_L	temperature of atmosphere below fluid 1
T_U	temperature of atmosphere above fluid 2
$\overline{T_W}$	wall dimensionless temperature
$\underline{T_W}$	wall temperature
$\Delta T = T_L - T_U$	atmosphere temperature difference
w	fluid 2 third component of velocity
w_1	fluid 1 third component of velocity
W	fluid 2 amplitude of third component of velocity
W_1	fluid 1 amplitude of third component of velocity

Greek Symbols

α_1	fluid 1 thermal diffusivity
α_2	fluid 2 thermal diffusivity
α_W	wall thermal diffusivity
α	fluid 1 over fluid 2 thermal diffusivities ratio
γ	surface tension
γ_T	fluid 1 over fluid 2 ratio of surface tension derivatives with respect to temperature
ε	expansion parameter
μ	fluid 1 over fluid 2 dynamic viscosities ratio
μ_1	fluid 1 dynamic viscosity
μ_2	fluid 2 dynamic viscosity
ν_1	fluid 1 kinematic viscosity
ν_2	fluid 2 kinematic viscosity
ρ	fluid 1 over fluid 2 densities ratio
ρ_1	fluid 1 density
ρ_2	fluid 2 density
ρ_W	wall density
Σ	real part: growth rate; negative imaginary part: frequency
σ	real part of Σ growth rate
σ_0, σ_1	scaled σ's at different orders

NOMENCLATURE *(continued)*

τ	fluid 2 temperature amplitude	τ_W	wall temperature amplitude
τ_1	fluid 1 temperature amplitude	χ	wall over fluid 2 thermal diffusivities ratio

Kechil and Hashim (2009). The problem in a cylindrical geometry was investigated by Dávalos-Orozco and You (2000) and for a viscoelastic fluid by Moctezuma-Sánchez and Dávalos-Orozco (2015).

More realistic conditions for thermocapillary instability are taken into account when the solid boundary is assumed to have finite thickness and thermal conductivity. These are considered by Takashima (1970), by Yang (1992) with buoyancy effects, and by Char and Chen (1999) for temperature-dependent viscosity. Besides, a nonuniform temperature gradient is assumed by Gangadharaiah (2013) and viscoelastic effects are introduced by Hernández-Hernández and Dávalos-Orozco (2015). For the case of liquid films falling down walls see Davalos-Orozco (2012, 2014, 2015, 2016).

It is of interest that Catton and Lienhard (1984) and Lienhard and Catton (1986) investigated the natural convection of a system with two liquid layers separated by a solid interlayer. They found that there are conditions where one of the liquid layers stays in a hydrostatic situation when the other one shows natural convection instability. However, under other conditions both layers can be unstable, depending in particular on the thickness and conductivity of the solid interlayer.

It is the goal of the present paper to investigate the linear thermocapillary interaction of two thin liquid layers coating both sides of a solid interlayer in the absence of gravity. As can be seen in the author's references reviewed above, it has been of interest for some years to take into account the presence of a thick wall to obtain results closer to experimental conditions (see in particular Hernández-Hernández and Dávalos-Orozco, 2015). However, also of concern is the presence of another liquid layer located on the other side of the wall (due, for example, to the coating of both sides of a solid plate, for instance, by dip-coating or due to condensation). The influence of this extra liquid layer on the thermocapillary stability of the whole system is the new subject of this paper. The system is subjected to a temperature gradient due to the temperature difference between the atmospheres present outside the free surface of each of the two fluid layers. Systems with two free surfaces have been investigated in the past. For example, Oron et al. (1995a,b) investigated the thermocapillary instability of a liquid sheet under a temperature gradient with a flat and a deformable surface, respectively. Davalos-Orozco (1999) calculated the thermocapillary instability of a liquid sheet in motion with deformable free surfaces. This instability has also been investigated by Fu et al. (2013) and by Tong et al. (2014) for a viscoelastic fluid. The case when the liquid layer is coating a deformable membrane is discussed in Dávalos-Orozco (2001).

An assumption in the present paper is that the free surfaces are flat as done by Pearson (1958) and that the corresponding Biot numbers are very small. The first assumption can be satisfied by fluids with a very large surface tension number defined as $S = \gamma_1 d_1/\rho_1\nu_1\alpha_1$, where γ_1 is the surface tension, d_1 is the thickness of the layer, ρ_1 is the density, ν_1 is the kinematic viscosity, and α_1 is the thermal diffusivity, all of fluid 1. Liquids like silicon oils have a very large S (see Al-Sibai et al., 2002). For example, with γ_1 = 0.0187 kg/sec^2, ρ_1 = 870 kg/m^3, $\nu_1 = 2.1609 \times 10^{-6}$ m^2/sec, $\alpha_1 = 2.1609 \times 10^{-7}$ m^2/sec with Prandtl number = 10 and for a liquid layer thickness d_1 = 0.001 m, $S = 4.60304 \times 10^4$. The possibility of small Biot numbers is demonstrated in Kabova and Kuznetsov (2002) and Kabova et al. (2006) from experimental data. This last assumption affects Marangoni convection in such a way that convection cells are very large, as calculated by Pearson (1958), where the wave number tends to zero. The small wave-number approximation has been applied in natural convection by Hurle et al. (1967); Chapman and Proctor (1980); Proctor (1981); Dávalos (1984); Dávalos and Manero (1986); and Pérez-Reyes and Dávalos-Orozco (2014).

Natural convection in a two-layer system has been investigated by Nepomnyashchy and Simanovskii (1983, 1984, 1985, 1986). See a complete review in Nepomnyashchy et al. (2012). However, particular attention is given to the work on natural convection for a two-fluid system with a flat free surface and a flat fluid-fluid interface investigated

by Gershuni and Zhukhovitskii (1986). The reason is that these authors use a small Biot number approximation in the problem. Some characteristics of their results are similar to those obtained in this paper for Marangoni convection, as will be shown presently. Notice that the small Biot and wave-number approximation was also used for thermocapillary convection in a liquid sheet with flat surfaces by Oron et al. (1995a).

Here the small wave-number approximation is applied up to fourth order in the wave-number expansion of the variables. This is a new procedure under this approximation. It is important to point out that the expansion is usually done up to second order in the wave-number expansion. The goal is to be able to capture the minimum of the marginal Marangoni numbers (that is, the critical Marangoni number Ma_C) with critical wave number k_C of both zero and finite magnitude. Besides, it is of interest to calculate the wave number of the maximum growth rate $\mathrm{k}_{\max}$ in regions where the critical wave number is zero and different from zero. Notice that by definition, the marginal curves and in particular the critical point occur when the growth rate of the perturbations is zero. A slight increase from criticality of the Marangoni number leads to a temporal growth of the perturbations. As will be seen presently, the number of parameters is very large and therefore some of them will be fixed. A variety of plots of Ma_C, k_C, and $k_{\max}$ against some parameters of the problem are presented in order to understand the behavior of this complex system.

The paper is organized as follows. The next section presents the description of the system and the corresponding equations of motion and heat transfer of the two fluids and the solid interlayer. The numerical results are given in Section 3. Section 4 presents the conclusions.

2. EQUATIONS OF MOTION

The goal of this paper is to investigate the thermocapillary stability of a system composed of two liquid layers coating both sides of a solid wall in the absence of gravity. The wall and liquid layers extend to infinity in the horizontal directions. The free surfaces are assumed to be flat and calculations are done in the same way as Pearson (1958). This system is sketched in nondimensional form in Fig. 1 where fluid 2 has thickness 1 and fluid 1 has thickness d. The wall has thickness d_W. The dashed lines are the free surfaces of each fluid and they are exposed to the ambient atmospheres which have different temperatures. In the figure, the atmosphere below fluid 1 is hotter than that above fluid 2, but the contrary may also be possible because gravity is not present in this problem. This situation can produce Marangoni instability in one of the two layers after a large enough temperature difference is reached between the atmospheres. However, the perturbations of the unstable liquid layer can influence the stable one due to the thermal interaction they have through the thick wall.

The system of equations corresponds to the equations of motion of the two fluids and the equations of heat transfer of the wall and the two fluids, all of them with their corresponding boundary conditions. They are made nondimensional as follows. The distance is measured with d_2 the thickness of fluid 2; time with d_2^2/α_2, where α_2 is the thermal diffusivity of fluid 2; velocity with α_2/d_2; and pressure with $\rho_2\alpha_2\nu_2/d_2^2$, where ν_2 is the kinematic viscosity

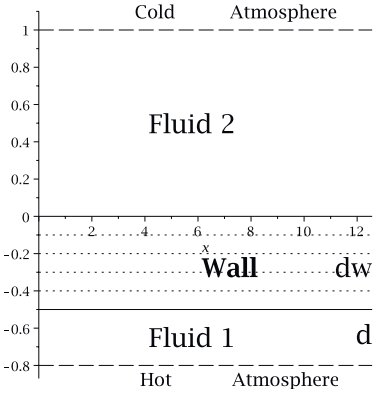

FIG. 1: Sketch of the system in nondimensional form. Two fluid layers coating both sides of a solid interlayer in the absence of gravity. The free surfaces are assumed flat and with different temperature

of fluid 2. The temperature is scaled with $\Delta T = (T_L - T_U)/den$, where T_L is the temperature of the atmosphere below fluid 1 and T_U is the temperature of the atmosphere above fluid 2. The denominator is defined as

$$den = \frac{d}{K} + \frac{d_W}{\chi} + 1. \tag{1}$$

Here, $d = d_1/d_2$, where d_1 and d_2 are the thicknesses of fluid 1 and fluid 2, respectively. $d_W = \overline{d_W}/d_2$, where $\overline{d_W}$ is the thickness of the wall. $K = K_1/K_2$, where K_1 and K_2 are the thermal conductivities of fluid 1 and fluid 2, respectively. $\chi = K_W/K_2$, where K_W is the thermal conductivity of the wall.

The nondimensional equations of motion, heat transfer, and continuity of fluid 2 are

$$\frac{1}{\mathrm{Pr}}\frac{d\overrightarrow{V}}{dt} = -\nabla P + \nabla^2 \overrightarrow{V}, \tag{2}$$

$$\frac{d\overline{T}}{dt} = \nabla^2 \overline{T}, \tag{3}$$

$$\nabla \cdot \overrightarrow{V} = 0, \tag{4}$$

where $\overrightarrow{V}$ is the velocity vector, P is the pressure, $\overline{T} = den\,(\underline{T} - T_U)/(T_L - T_U)$ is the temperature, $\underline{T}$ is the dimensional temperature, and $d/dt = \partial/\partial t + \overrightarrow{V} \cdot \nabla$ is the Lagrange operator of fluid 2. The Prandtl number is defined as $\mathrm{Pr} = \nu_2/\alpha_2$.

The equations of fluid 1 are

$$\frac{1}{\mathrm{Pr}}\frac{d^*\overrightarrow{V_1}}{dt} = -\frac{1}{\rho}\nabla P_1 + \frac{\mu}{\rho}\nabla^2 \overrightarrow{V_1}, \tag{5}$$

$$\frac{d^*\overline{T_1}}{dt} = \alpha \nabla^2 \overline{T_1}, \tag{6}$$

$$\nabla \cdot \overrightarrow{V_1} = 0, \tag{7}$$

where $\overrightarrow{V_1}$ is the velocity vector, P_1 is the pressure, $\overline{T_1} = den\,(\underline{T_1} - T_U)/(T_L - T_U)$ is the temperature, $\underline{T_1}$ is the dimensional temperature of fluid 1, and $d^*/dt = \partial/\partial t + \overrightarrow{V_1} \cdot \nabla$ is the Lagrange operator of fluid 1. μ is the ratio μ_1/μ_2, where μ_1 is the dynamic viscosity of fluid 1 and $\rho = \rho_1/\rho_2$, where ρ_1 is the density of fluid 1. The ratio $\alpha = \alpha_1/\alpha_2$, where α_1 is the thermal diffusivity of fluid 1, can also be written as

$$\alpha = \frac{K}{\rho(c_{P1}/c_{P2})}.$$

The heat capacities of fluid 1, fluid 2, and the wall are c_{P1}, c_{P2}, and c_{PW}, respectively. The heat diffusion equation of the wall is

$$\frac{\partial \overline{T_W}}{\partial t} = \frac{\alpha_W}{\alpha_2}\nabla^2 \overline{T_W}. \tag{8}$$

Here $\overline{T_W} = den\,(\underline{T_W} - T_U)/(T_L - T_U)$ is the wall temperature, α_W is the wall thermal diffusivity, and $\underline{T_W}$ is the dimensional temperature of the wall. The ratio of diffusivities can also be expressed as

$$\frac{\alpha_W}{\alpha_2} = \chi \Big/ \left(\frac{\rho_W}{\rho_2}\frac{c_{PW}}{c_{P2}}\right),$$

where ρ_W is the density of the wall.

The main temperature profiles (defined without bars) of the system are calculated under hydrostatic conditions. Their boundary conditions (see Fig. 1) in nondimensional form are the following.

$$\overline{T} = 0 \quad \text{at} \quad z = 1 \tag{9}$$

$$\overline{T} = \overline{T_W} \quad \text{and} \quad \frac{d\overline{T}}{dz} = \chi \frac{d\overline{T_W}}{dz} \quad \text{at} \quad z = 0 \tag{10}$$

$$\overline{T_W} = \overline{T_1} \quad \text{and} \quad \frac{\chi}{K}\frac{d\overline{T_W}}{dz} = \frac{d\overline{T_1}}{dz} \quad \text{at} \quad z = -d_W \tag{11}$$

$$\overline{T_1} = den \quad \text{at} \quad z = -d_W - d \tag{12}$$

The nondimensional solutions of the main temperatures of fluid 2, the wall, and fluid 1 are, respectively,

$$T(z) = 1 - z, \tag{13}$$

$$T_W(z) = 1 - \frac{z}{\chi}, \tag{14}$$

$$T_1(z) = den - \frac{1}{K}(z + d_W + d). \tag{15}$$

To calculate the linear equations satisfied by the fluid velocities perturbations, the equations of motion of fluid 1 and fluid 2 are operated twice by the rotational operator or rotor ($\nabla\times$). Now, the linear heat diffusion equations only contain the vertical component of velocity of the corresponding fluid 1 or 2 (see below). Therefore, it is found that only the third components of the equations obtained from the rotational operations are coupled to their corresponding thermal diffusion equation. Those components only contain the third component of velocity. Thus, w and w_1 are defined as the third components of the velocity perturbations of fluid 2 and fluid 1, respectively. Moreover, use is made of normal modes for the velocities and temperatures of fluid 1, fluid 2, and the wall. In this case (w, w_1, $\overline{T}$, $\overline{T_W}$, $\overline{T_1}$) have the form (W, W_1, τ, τ_W, τ_1) $\exp[i(k_x x + k_y y) + \Sigma t]$, where ($W$, W_1, τ, τ_W, τ_1) only depend on z and represent the amplitudes of the velocity and temperature perturbations. The meaning of these normal modes is that the infinite plane is filled with tessellated horizontal structures. The Σ = Re(Σ) + i Im(Σ) is a complex number whose real part Re(Σ) is the growth rate and its imaginary part Im(Σ) is the frequency of oscillation. k_x and k_y are the x and y components of the wave-number vector. In normal modes the Laplacian operator changes into $\nabla^2 \to D^2 - k^2$ and the time partial derivative into $\partial/\partial t \to \Sigma$, where the definitions $D = d/dz$ and $k^2 = k_x^2 + k_y^2$ are used. In what follows, the magnitude of the wave number is scaled as $k = \varepsilon k_S$, where k_S is the order one scaled wave number and ε is the expansion parameter which satisfies $\varepsilon \ll 1$. The calculations presented below were also done including the frequency of oscillation Im(Σ) [in the marginal state with Re(Σ) = 0] and it was found that the frequency needed to make zero the imaginary part of the marginal Marangoni number is zero. Therefore, in order to calculate the most dangerous mode of instability, it is assumed that in nonoscillatory convection, the growth rate is scaled as Re(Σ) = $\sigma = \varepsilon^4 (\sigma_0 + \varepsilon^2 \sigma_1)$.

In this way, by use of the main temperature profiles the linear perturbation equations for fluid 2 are

$$\frac{1}{\mathrm{Pr}}\varepsilon^4(\sigma_0 + \varepsilon^2\sigma_1)\left(D^2 - \varepsilon^2 k_S^2\right) W - \left(D^2 - \varepsilon^2 k_S^2\right)^2 W = 0, \tag{16}$$

$$\varepsilon^4(\sigma_0 + \varepsilon^2\sigma_1)\tau - W = \left(D^2 - \varepsilon^2 k_S^2\right)\tau, \tag{17}$$

for fluid 1,

$$\frac{1}{\mathrm{Pr}}\varepsilon^4(\sigma_0 + \varepsilon^2\sigma_1)\left(D^2 - \varepsilon^2 k_S^2\right) W_1 - \frac{\mu}{\rho}\left(D^2 - \varepsilon^2 k_S^2\right)^2 W_1 = 0, \tag{18}$$

$$\varepsilon^4(\sigma_0 + \varepsilon^2\sigma_1)\tau_1 - \frac{1}{K}W = \left(D^2 - \varepsilon^2 k_S^2\right)\tau_1, \tag{19}$$

and for the wall,

$$\varepsilon^4(\sigma_0 + \varepsilon^2\sigma_1)\tau_W = \frac{\alpha_W}{\alpha_2}\left(D^2 - \varepsilon^2 k_S^2\right)\tau_W. \tag{20}$$

Next, we address the boundary conditions for the velocities and the temperatures. The free surfaces are assumed flat and the components of the velocities of fluid 1 and fluid 2 perpendicular to the surface have to be zero.

$$D\tau = -\mathrm{Bi}\tau, \quad W = 0, \quad D^2 W = -\mathrm{Ma}\varepsilon^2 k_S^2 \tau \quad \text{at} \quad z = 1, \tag{21}$$

$$\tau = \tau_W, \quad D\tau = \chi D\tau_W, \quad W = 0, \quad DW = 0 \quad \text{at} \quad z = 0, \tag{22}$$

$$\tau_W = \tau_1, \quad \frac{\chi}{K} D\tau_W = D\tau_1, \quad W_1 = 0, \quad DW_1 = 0 \quad \text{at} \quad z = -d_W, \tag{23}$$

$$D\tau_1 = \frac{\text{Bi}_1}{d}\tau_1, \quad W_1 = 0, \quad D^2 W_1 = \gamma_T \text{Ma}\varepsilon^2 k_S^2 \tau_1 \quad \text{at} \quad z = -d_W - d. \tag{24}$$

Bi = $\text{H}_{h2}d_2/K_2$ and $\text{Bi}_1 = \text{H}_{h1}d_1/K_1$ are the Biot numbers of fluid 2 and fluid 1, respectively. H_{h2} and H_{h1} are the coefficients of heat transfer across the free surfaces of fluid 2 and fluid 1, respectively. Notice that $\text{Bi}_1/d = \text{H}_{h1}d_2/K_1$. The Marangoni number is defined as

$$\text{Ma} = -\frac{d\gamma}{dT}\frac{\Delta T}{den}\frac{d_2}{\rho_2 \nu_2 \alpha_2}, \tag{25}$$

where γ is the surface tension of fluid 2 and $d\gamma/dT < 0$ is the derivative of that surface tension with respect to temperature which is negative for most fluids. $\gamma_T = (d\gamma_1/dT)/(d\gamma/dT)$ is the ratio of the derivative of surface tension with respect to temperature of fluid 1 over that of fluid 2.

Here it is assumed that the Biot numbers are very small. In this case, very large scale convection cells are formed and the flow is very slow (see Pearson, 1958). Therefore, the wave number is very small, too, and it will be used as an expansion parameter, in the form $\varepsilon k_S \ll 1$ with k_S order one. In this way, the Biot numbers are scaled as Bi = $\varepsilon^4 k_S^4$ bi and $\text{Bi}_1 = \varepsilon^4 k_S^4$ bi_1, where bi and bi_1 are of order one.

It is of interest here to calculate Ma corresponding to the marginal state of the system where the real part Re(Σ) = σ = 0, that is, zero growth rate. It is also of interest to calculate the wave number $k_{\max}$ corresponding to the maximum growth rate when the Marangoni number is slightly above the marginal state and $\sigma > 0$. Recall that the calculations presented below were done with Im(Σ) [and Re(Σ) = 0] and it was found that the frequency needed to make zero the imaginary part of the marginal Marangoni number is zero. That is, under the present approximation in the marginal state, Σ should always be zero and the flow is stationary.

In the equations and boundary conditions the exponent of the wave number k is always even. Therefore the following expansion of the variables is made, taking into account that the flow motion is slow.

$$W = \varepsilon^2 W_0 + \varepsilon^4 W_1 + \varepsilon^6 W_2 + \cdots \quad \tau = \tau_0 + \varepsilon^2 \tau_1 + \varepsilon^4 \tau_2 + \cdots, \tag{26}$$

$$W_1 = \varepsilon^2 W_{10} + \varepsilon^4 W_{11} + \varepsilon^6 W_{12} + \cdots \quad \tau_1 = \tau_{10} + \varepsilon^2 \tau_{11} + \varepsilon^4 \tau_{12} + \cdots, \tag{27}$$

$$\tau_W = \tau_{W0} + \varepsilon^2 \tau_{W1} + \varepsilon^4 \tau_{W2} + \cdots \quad \text{Ma} = \text{Ma}_0 + \varepsilon^2 \text{Ma}_{1S} + \varepsilon^4 \text{Ma}_{2S} + \cdots. \tag{28}$$

The marginal Marangoni number is calculated up to fourth order in k using the Maple algebra package. This allows us to find a critical Marangoni number with a corresponding finite critical wave number when the Biot numbers are very small but different from zero. There are also conditions under which k_C can be zero. This means that the convection cell is very large and will fill the whole liquid layers. The algebraic calculations are very long, complex, and tedious and will not be presented here. The procedure is similar to that found in the literature for natural convection (Hurle et al., 1967; Chapman and Proctor, 1980; Proctor, 1981; Dávalos-Orozco, 1984; Dávalos-Orozco and Manero, 1986; Gershuni and Zhukhovitskii, 1986; Pérez-Reyes and Dávalos-Orozco, 2014) and for a liquid sheet with flat free surfaces (Oron et al., 1995a). It will be shown presently that the scaled $\text{Ma}_{1S} = k_S^2$ Ma_1 and the scaled $\text{Ma}_{2S} = k_S^4$ Ma_2. Thus, using the identity $k = \varepsilon k_S$, the calculated marginal Marangoni number has the form

$$\text{Ma} = \text{Ma}_0 + k^2 \text{Ma}_1 + k^4 \text{Ma}_2. \tag{29}$$

The coefficients Ma_0, Ma_{1S}, and Ma_{2S} were obtained from the first, second, and third solvability conditions, respectively (see the Appendix). Here,

$$\text{Ma}_0 = \frac{48\alpha(\chi d_W + dK + 1)}{\alpha - d^3\gamma_T}, \tag{30}$$

and

$$\begin{aligned}\mathrm{Ma}_1 = \frac{16}{5K\chi d}\frac{\alpha}{(\alpha - d^3\gamma_T)^3}\Big[&K^2\chi d^{10}\gamma_T^2 - 3\chi K\gamma_T^2\left(\chi d_W + 1\right)d^9 - 9\chi\gamma_T^2\left(\chi d_W + 1\right)^2 d^8 - 5K\gamma_T\big[d_W\gamma_T \\ &\times\left(\chi^2 d_W^2 + 3\chi d_W + 3\right) + \chi\left(K\alpha + \gamma_T\left(1 - 3\mathrm{bi}\right)\right)\big]d^7 - 15K\chi\gamma_T\big[\alpha\left(\chi d_W + 1\right) - K\mathrm{bi}_1\gamma_T\big]d^6 \\ &- 15K^2\alpha\gamma_T\big[dw^2\chi + \chi + 2d_W\big]d^5 - 5\alpha K\chi\big[d_W\gamma_T\left(\chi d_W^2 + 3d_W + 3\chi\right) + \left(K\alpha + \left(1 + 6\mathrm{bi}\right)\gamma_T\right)\big]d^4 \\ &- 3\alpha K^2\big[5\alpha K d_W + \left(3\alpha K + 10\mathrm{bi}_1\gamma_T\right)\chi\big]d^3 - 3\alpha^2k^2\chi\big[5d_W^2 + 6\chi d_W + 1\big]d^2 \\ &- K\chi\alpha^2\big[5\chi K d_W^3 + 9\chi^2 d_W^2 + 3\chi d_W - 15\mathrm{bi} - 1\big]d + 15K^2\chi\mathrm{bi}_1\alpha^2\Big].\end{aligned} \tag{31}$$

The number of terms in Ma_2 is very large and will not be presented here. These Ma_0 and Ma_1 show a characteristic common to Ma_2. That is, the denominator $\alpha - d^3\gamma_T$. The marginal Marangoni number can be written as

$$\mathrm{Ma} = \frac{\overline{\mathrm{Ma}_0}}{\alpha - d^3\gamma_T} + k^2\frac{\overline{\mathrm{Ma}_1}}{(\alpha - d^3\gamma_T)^3} + \frac{\overline{\mathrm{Ma}_2}}{(\alpha - d^3\gamma_T)^5}k^4, \tag{32}$$

where $\overline{\mathrm{Ma}_0}$, $\overline{\mathrm{Ma}_1}$, and $\overline{\mathrm{Ma}_2}$ are the Marangoni coefficients without their corresponding denominators. It is interesting that this denominator is similar to that found by Gershuni and Zhukhovitskii (1986) in natural convection with an interface and a free surface in a stratified two-layer system. It depends on the fluid properties and fluid layer's relative thicknesses. Notice here that the powers of the denominators are odd. This brings about the possibility of having negative marginal and critical Marangoni numbers when, according to the magnitudes of the parameters involved, the sign of $\alpha - d^3\gamma_T$ is changed.

The minimum of Eq. (29) is calculated taking the derivative with respect to k. A third-order algebraic equation is obtained for k. Two non-negative critical wave numbers are possible, k_C = 0 and $k_C^2 = -\,\mathrm{Ma}_1/2\,\mathrm{Ma}_2$. Substitution of k_C in Eq. (29) gives the critical Marangoni number $\mathrm{Ma}_C = \mathrm{Ma}_0 - \mathrm{Ma}_1^2/4\,\mathrm{Ma}_2$ (for $k_C > 0$) and $\mathrm{Ma}_C = \mathrm{Ma}_0$ (for $k_C = 0$). In the last k_C the sign of $\alpha - d^3\gamma_T$ has no effect because the ratio has $(\alpha - d^3\gamma_T)^2$ in the resulting numerator. In case k_C is imaginary then the the critical wave number is k_C = 0. Thus it can be shown that k_C = 0 corresponds to a maximum of Ma when $\mathrm{Ma}_1 < 0$ and to a minimum when $\mathrm{Ma}_1 > 0$. The contrary occurs when $k_C > 0$. In this case, k_C corresponds to a maximum of Ma when $\mathrm{Ma}_1 > 0$ and to a minimum when $\mathrm{Ma}_1 < 0$.

The critical Marangoni number and the corresponding critical wave number are calculated numerically as follows. First, all the parameters except one are fixed and each Ma_0, Ma_1, and Ma_2 are evaluated varying the parameter left. In this way, it is possible to present the plots of Ma_C and k_C in the figures of the next section.

The possibility of k_C = 0 is found immediately in a particular case where the thickness of fluid 1 and the heat conductivity of the wall tend to zero (fluid 1 does not exist). That is, when $d \to 0$ and $\chi \to 0$ in Ma_0, to get Ma_C = 48. This value was first obtained by Pearson (1958) in the limit when both Biot numbers and the wave number tend to zero.

The physical meaning of a critical wave number k_C = 0 is that one convection cell is extremely large and can fill the whole liquid layer. In this case, the marginal curve of Ma has the form of a parabola with respect to k which has its vertex (its minimum) located at k = 0.

When the system is slightly above the marginal state, the amplitude of the unstable convection cells grows with time. As explained above this growth is represented by the growth rate $\sigma = \varepsilon^4\left(\sigma_0 + \varepsilon^2\sigma_1\right)$. The second term $\varepsilon^6\sigma_1$ is extremely large and will not be presented here. Thus, only the first one is given below.

$$\begin{aligned}\varepsilon^4\sigma_0 = (1/48)\Big\{&[k^2\left(\alpha - d^3\gamma_T\right)\varepsilon^2\mathrm{Ma}_{1S}]/[dK + \alpha + (\rho_W/\rho_2)(cp_W/cp_2)d_W\alpha]\Big\} \\ &- \left\{(k^4\alpha)\Big/\left[15K\chi d\left(dK + \alpha + \frac{\rho_W}{\rho_2}\frac{cp_W}{cp_2}d_W\alpha\right)\left(\alpha - d^3\gamma_T\right)^2\right]\right\}\Big[K^2\chi d^{10}\gamma_T^2 - 3\chi K\gamma_T^2\left(\chi d_W + 1\right) \\ &\times d^9 - 9\chi\gamma_T^2\left(\chi d_W + 1\right)^2 d^8 - 5K\gamma_T\big[d_W\gamma_T\left(\chi^2 d_W^2 + 3\chi d_W + 3\right) + \chi\left(K\alpha + \gamma_T\left(1 - 3\mathrm{bi}\right)\right)\big]d^7 \\ &- 15K\chi\gamma_T \times \big[\alpha\left(\chi d_W + 1\right) - K\mathrm{bi}_1\gamma_T\big]d^6 - 15K^2\alpha\gamma_T\big[dw^2\chi + \chi + 2d_W\big]d^5 - 5\alpha K\chi\big[d_W\gamma_T \\ &\times\left(\chi d_W^2 + 3d_W + 3\chi\right) + \left(K\alpha + \left(1 + 6\mathrm{bi}\right)\gamma_T\right)\big]d^4 - 3\alpha K^2\big[5\alpha K d_W + \left(3\alpha K + 10\mathrm{bi}_1\gamma_T\right)\chi\big]d^3 \\ &- 3\alpha^2k^2\chi\big[5d_W^2 + 6\chi d_W + 1\big]d^2 - K\chi\alpha^2\big[5\chi K d_W^3 + 9\chi^2 d_W^2 + 3\chi d_W - 15\mathrm{bi} - 1\big]d + 15K^2\chi\mathrm{bi}_1\alpha^2\Big].\end{aligned} \tag{33}$$

This equation may be expressed as

$$\varepsilon^4\sigma_0 = \left\{1\Big/\left(dK+\alpha+\frac{\rho_W}{\rho_2}\frac{cp_W}{cp_2}d_W\alpha\right)\right\}\left(\frac{A_1}{\left(\alpha-d^3\gamma_T\right)^2}k^4+B_1\left(\alpha-d^3\gamma_T\right)k^2\varepsilon^2\mathrm{Ma}_{1S}\right), \tag{34}$$

where A_1 and B_1 depend on the parameters of the problem but not on k and Ma_{1S}. In this case, the small magnitude of $\varepsilon^2\mathrm{Ma}_{1S}$ has to be given to be slightly above the critical Ma_C. It is important to note that $\varepsilon^4\sigma_0$ is useful only to describe the growth rate in the region where the critical wave number is $k_C = 0$. The $\varepsilon^6\sigma_1$ is useful for the growth rate when $k_C > 0$ as will be seen presently. It has the form

$$\varepsilon^6\sigma_1 = \left[1\Big/\left(dK+\alpha+\frac{\rho_W}{\rho_2}\frac{cp_W}{cp_2}d_W\alpha\right)\right]\left(\frac{A_2}{\left(\alpha-d^3\gamma_T\right)^4}k^6+B_2\left(\alpha-d^3\gamma_T\right)k^2\varepsilon^4\mathrm{Ma}_{2S}\right), \tag{35}$$

where A_2 and B_2 depend on the parameters of problem but not on k and Ma_{2S}. In the following section the graphs of $\varepsilon^4\sigma_0$ and $\varepsilon^6\sigma_1$ are not presented. Instead, the graphs of the most dangerous mode are presented for $k_{\max}$. The formula of $k_{\max}$ from Eq. (34) is valid when $k_C = 0$ has the form

$$k_{\max} = \left(-\frac{B_1\left(\alpha-d^3\gamma_T\right)^3\varepsilon^2\mathrm{Ma}_{1S}}{2A_1}\right)^{1/2}. \tag{36}$$

It is useful when the radicand is positive. The formula of $k_{\max}$ from Eq. (35) is valid when $k_C > 0$ has the form

$$k_{\max} = \left(-\frac{B_2\left(\alpha-d^3\gamma_T\right)^5\varepsilon^4\mathrm{Ma}_{2S}}{3A_2}\right)^{1/4}. \tag{37}$$

Again, it is useful when the radicand is positive. Observe that both growth rates require the wall over fluid 2 densities and heat capacities ratios ρ_W/ρ_2 and cp_W/cp_2, respectively. However, the term containing them simplifies when calculating both $k_{\max}$'s of Eqs. (36) and (37), which are required below to describe the most unstable mode of instability. That term also simplifies when calculating Ma_{1S} and Ma_{2S}. Results of the numerical analysis of Ma in Eq. (29) are presented in the following section along with those of Eq. (37) [and Eq. (36) when needed].

3. NUMERICAL RESULTS OF Ma IN EQ. (29)

In this section numerical results of Eq. (29) for the marginal and critical Marangoni number are calculated. The number of parameters is very large and some of them will be fixed to understand in an easier way the behavior of the critical Marangoni number under different conditions. First it will be assumed that both fluids and their corresponding atmospheres are the same. In that case, it is clear that $\mathrm{bi}_1/d = \mathrm{bi}$. Under this assumption the following parameters result, fixed through the paper: $\rho = K = \alpha = \gamma_T = 1$. In other words, the fluid densities, heat conductivities, heat diffusivities, and temperature derivatives of surface tension are all the same.

The variable parameters χ, bi, d_W, and d correspond to the wall-fluid heat conductivities ratio, the Biot number of fluid 2, the relative thickness of the wall, and the relative thickness of fluid 1, respectively. Under these assumptions, the term in the denominators of Eq. (32) becomes $1 - d^3$. It only depends on the relative thickness of fluid 1.

In particular, it is important to distinguish between the results for d smaller than 1 (thickness of fluid 2 larger than that of fluid 1) from those for d larger than 1 (thickness of fluid 2 thinner than that of fluid 1). Two separate graphs are given for these two cases.

Two samples of marginal curves are shown in Fig. 2. In Fig. 2(a) the parameters are $\chi = 0.1$, $d_W = 1$, $d = 0.1 < 1$, and the marginal Marangoni number is positive. Here, an increase of the Biot number, that is, the increase of the heat transfer across the free surface of fluid 2 changes the marginal curves in such a way that their minima, the critical points, move up and to the left and the critical wave number tends to zero. In Fig. 2(b) the parameters are bi = 0.1,

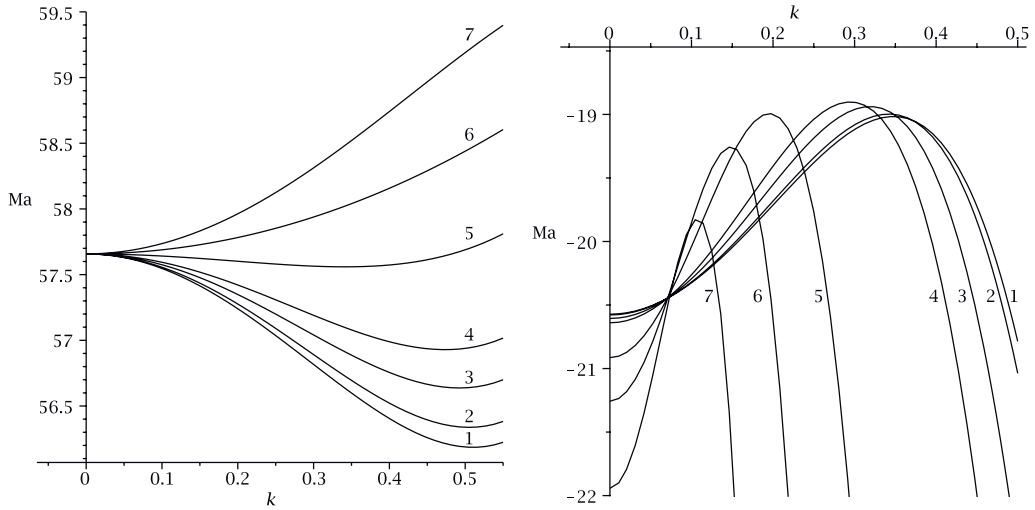

FIG. 2: Two sample figures with different types of marginal curves; (a) Ma vs k (χ = 0.1, d_W = 1, d = 0.1 $<$ 1), bi = (1) 0, (2) 0.01, (3) 0.03, (4) 0.05, (5) 0.1, (6) 0.15, (7) 0.2; (b) Ma vs k; negative Marangoni number (bi = 0.1, χ = 0.1, d = 2 $>$ 1), d_W = (1) 0.001, (2) 0.01, (3) 0.05, (4) 0.1, (5) 0.5, (6) 1, (7) 2

χ = 0.1, d = 2 $>$ 1. The marginal Marangoni number is negative. A characteristic of the minima of the curves (the points closer to the k axis) is that the change of the critical wave number is not monotonic with respect to an increase of d_W, the relative thickness of the wall.

Notice that the wave number of the minima of the marginal curves is $k \leq 0.5$ and that the Biot numbers are order one or less. Care is taken through the paper to satisfy these two conditions.

Now, the goal is to know the magnitude of the critical Marangoni number Ma_C, the corresponding critical wave number k_C, and $k_{\max}$, the wave number corresponding to the maximum growth rate (most dangerous mode). These are shown against the scaled Biot number for χ = 0.1, the relative heat conductivity of the wall, and d_W = 1, a wall thickness equal to that of fluid 2, in Fig. 3. Ma_C is presented in Fig. 3(a) against bi for different magnitudes of $d <$ 1, the relative thickness of fluid 1. The increase of Ma_C with bi is monotonic up to a magnitude where it becomes constant. This can be explained in Fig. 3(b) where it is found that at that particular bi and over, the critical wave number becomes zero. Notice that at k_C = 0, Ma in Eq. (29) always has the same magnitude, Ma_0, for the given parameters. The physical meaning is that the increase of heat transfer across the free surfaces is stabilizing only up to a magnitude where its effect is not important.

In contrast, as explained above, when the relative thickness of fluid 1, $d \to 0$, the decrease of bi leads to $k_C \to$ 0 if also $\chi \to 0$. This can be seen in the following asymptotic formula for small d where the relative thickness of the wall is d_W = 1:

$$\begin{aligned}\mathrm{Ma} = {} & 48\,(1+\chi) + \frac{16}{5}\left(1 + 30\mathrm{bi} - 8\chi - 9\chi^2\right)k^2 \\ & + \frac{16}{175}\left(3 - 420\mathrm{bi}(1+\chi) + 124\chi + 310\chi^2 + 189\chi^3\right)k^4 \\ & + \left[48 - \frac{288}{5}\,(1+\chi)\,k^2 + \frac{16}{175}\left(474 - \frac{1050\mathrm{bi}}{\chi} - 420\mathrm{bi} + 1040\chi + 567\chi^2\right)k^4\right]d.\end{aligned} \tag{38}$$

In this case for d_W = 1, the square of the critical wave number has the expression

$$k_C^2 = \frac{35\chi\left(1 + 30\mathrm{bi} - 9\chi^2 - 8\chi - 18d\chi - 18d\right)}{(840\chi\,(\chi + 1 + d) + 2100d)\,\mathrm{bi} - \chi\Omega}, \tag{39}$$

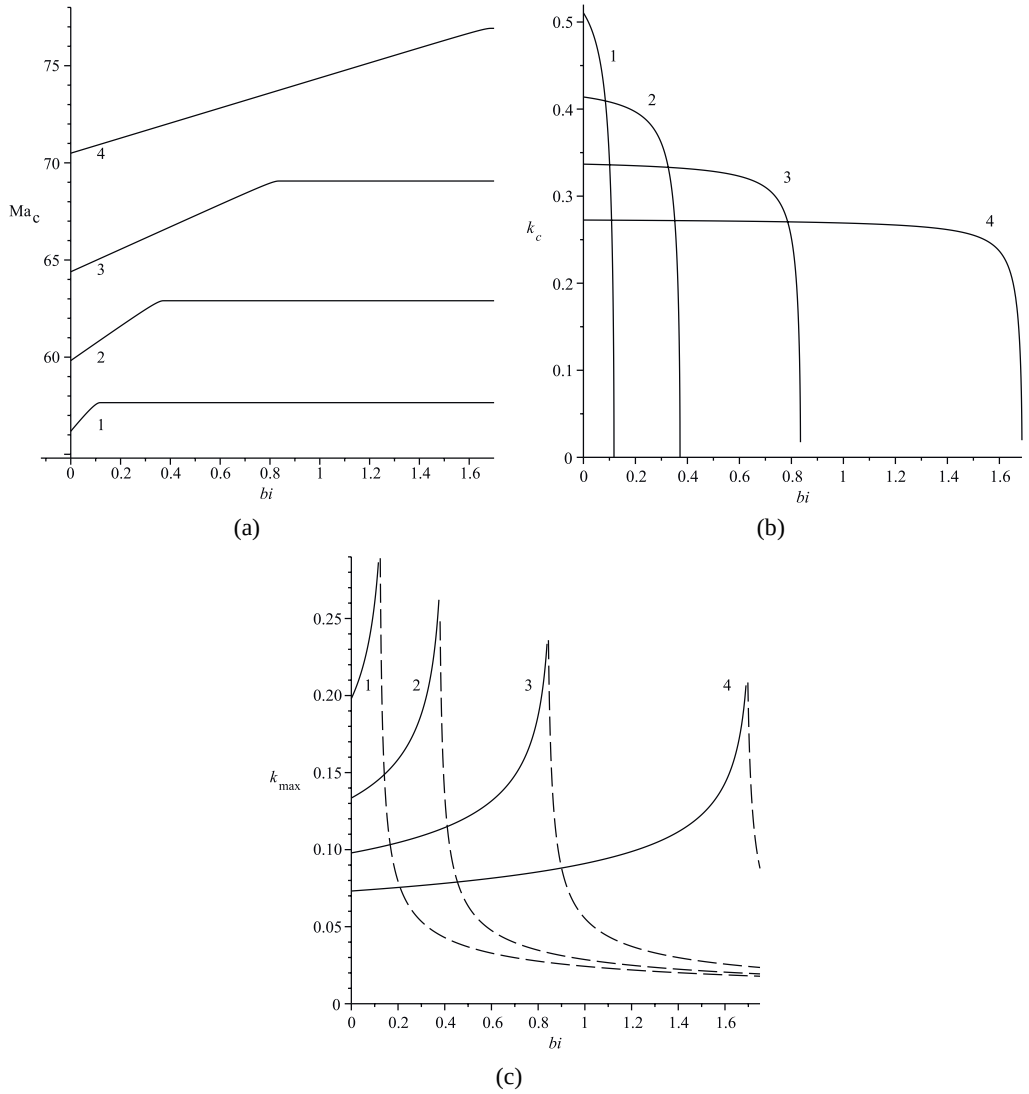

FIG. 3: χ = 0.1, d_W = 1; (a) Ma_C vs bi; (b) k_C vs bi; and (c) most dangerous mode $k_{\max}$ vs bi, solid when $k_C > 0$ (for $\varepsilon^4\mathrm{Ma}_{2S} = 0.1$) and dashed when k_C = 0 (for $\varepsilon^2\mathrm{Ma}_{1S} = 0.1$); d = (1) 0.1, (2) 0.2, (3) 0.3, (4) 0.4

where $\Omega = \left[378\chi^3 + (620 + 1134d)\chi^2 + (248 + 2080d)\chi + 6 + 948d\right]$. When bi = 0 one χ simplifies and the denominator of k_C^2 is negative. A condition for positive k_C^2 is that the numerator be negative. If k_C^2 is negative the critical wave number can only be zero. Therefore, in order to have k_C = 0, the numerator should be positive and one of the roots gives the condition $0 \leq \chi \leq 1/9 - 2d$. This means that it is still possible to have k_C = 0 when the relative conductivity of the wall χ is small but different from zero. Remember that d is assumed small in the formula. The case when bi $\neq$ 0 is a little more complex. It is interesting that under this situation the root corresponding to the previous case when bi = 0 does not give the needed condition for k_C = 0. Then, the other root of the numerator corresponding to positive χ now has the form $\chi_r = -d - 4/9 - (1/9)[(9d-5)^2 + 270\,\mathrm{bi}]^{1/2}$. The condition for k_C = 0 is that (*positive χ root of the denominator of k_C^2*) $< \chi \leq \chi_r$. In this region k_C^2 is always negative due to its denominator. Now, considering that χ is of the same order as d and that they tend to zero simultaneously, an expression for Ma is obtained containing bi and k alone. Under this assumption the critical wave number is always k_C = 0. The extrema obtained for k correspond to maxima (not minima) of Ma which, by the way, are outside the

small wave-number approximation. This example for small d only shows a facet of the whole complexity of the problem.

The curves of $k_{\max}$, the most dangerous mode, are presented in Fig. 3(c). The solid lines [Eq. (37) with $\varepsilon^4 \mathrm{Ma}_{2S}$ = 0.1] and the dashed lines [Eq. (36) with $\varepsilon^2 \mathrm{Ma}_{1S}$ = 0.1] correspond to $k_C > 0$ and k_C = 0 [see Fig. 3(b)], respectively. It is clear that a singularity occurs in both of the $k_{\max}$ at the bi where k_C drops to zero in Fig. 3(c).

Figure 4 presents results for $d > 1$. The thickness of fluid 1 is larger than that of fluid 2. In this case Ma_C is negative [see explanation of Fig. 2(b)]. The physical meaning is that the system is unstable only when the temperature of the atmosphere outside fluid 2 is larger than that of the atmosphere outside fluid 1. The fixed parameters are the relative conductivity of the wall χ = 0.1 and relative thickness of the wall d_W = 1. Graphs of the critical Marangoni number against the scaled Biot number are shown in Fig. 4(a). The curves for different d only vary slightly in the range of bi which has to be of order one. Therefore in this case the increase of heat transfer across the free surface is almost negligible. However, the influence that the relative thickness of fluid 1 has on the stability is clear. Plots of

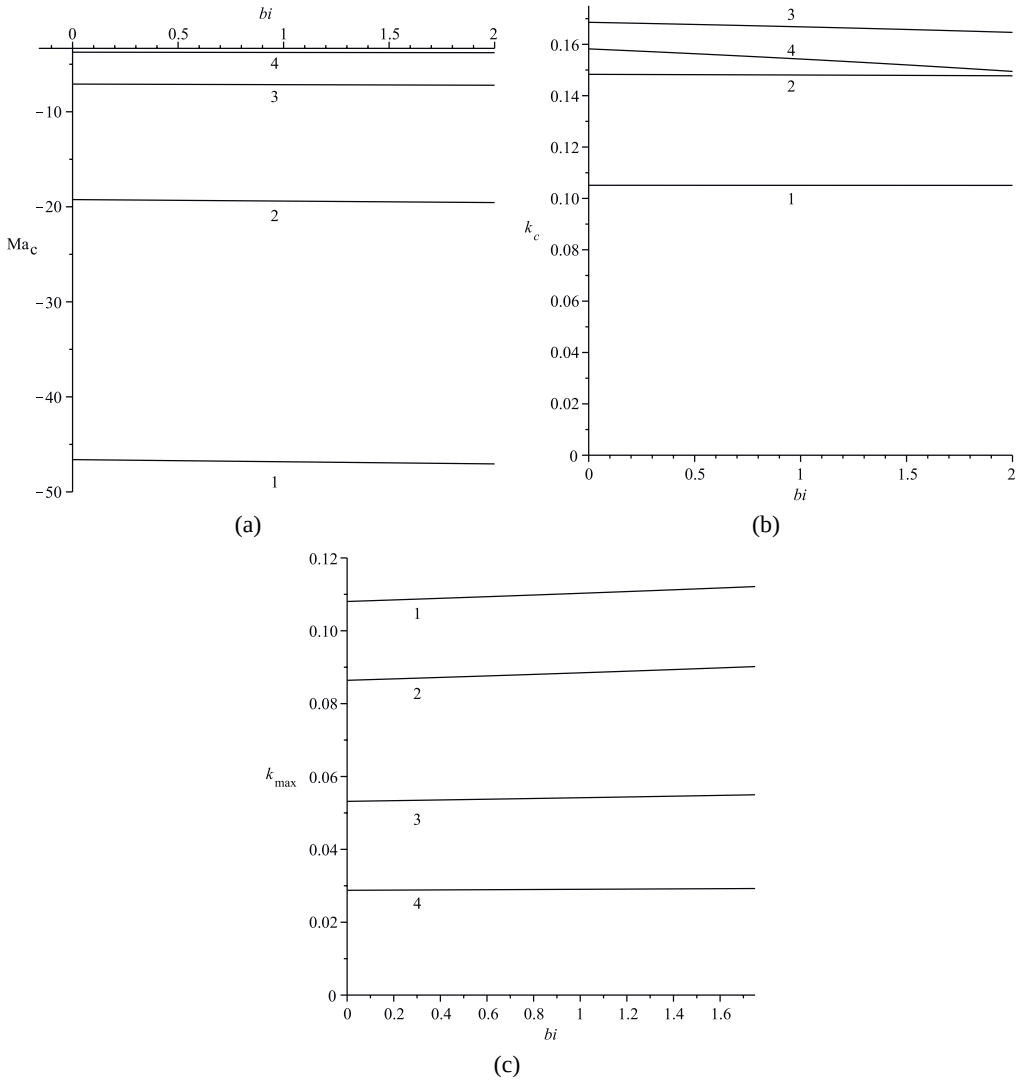

FIG. 4: χ = 0.1, d_W = 1; negative Ma_C; (a) Ma_C vs bi; (b) k_C vs bi; and (c) most dangerous mode $k_{\max}$ vs bi (for $\varepsilon^4 \mathrm{Ma}_{2S} = -0.1$); d = (1) 1.5, (2) 2, (3) 3, (4) 4

k_C vs bi are given in Fig. 4(b). Notice that the curve corresponding to d = 4 is below that of d = 3 and that it has a tendency to cross below the curve of d = 2. Figure 4(c) shows that the wave number of the most dangerous mode increases slowly but monotonically with bi. Notice in Eq. (37) that here $\varepsilon^4 \mathrm{Ma}_{2S}$ is negative. However, the sign is corrected with $1 - d^3$ which is also negative for $d > 1$.

Graphs of Ma_C, k_C, and $k_{\max}$ against χ (the relative heat conductivity of the wall) for bi = 0.1, d_W = 1 are plotted in Fig. 5. Here again the magnitude of d is smaller than 1. At first sight, the growth of Ma_C with respect to χ is monotonous in Fig. 5(a). However, it is not the case for $\chi < 0.1$ and d = 0.2, where χ has a destabilizing effect. Except for this case, the figure shows that the increase of the relative conductivity of the wall χ stabilizes.

The behavior of the curves of k_C vs χ is different as can be seen in Fig. 5(b). Each curve has a maximum (in some cases the maxima are above k = 0.5) after which the curves decrease. The physical meaning of this maximum is that the convection cells at criticality can have a minimum size, represented by their wavelength, for a certain magnitude

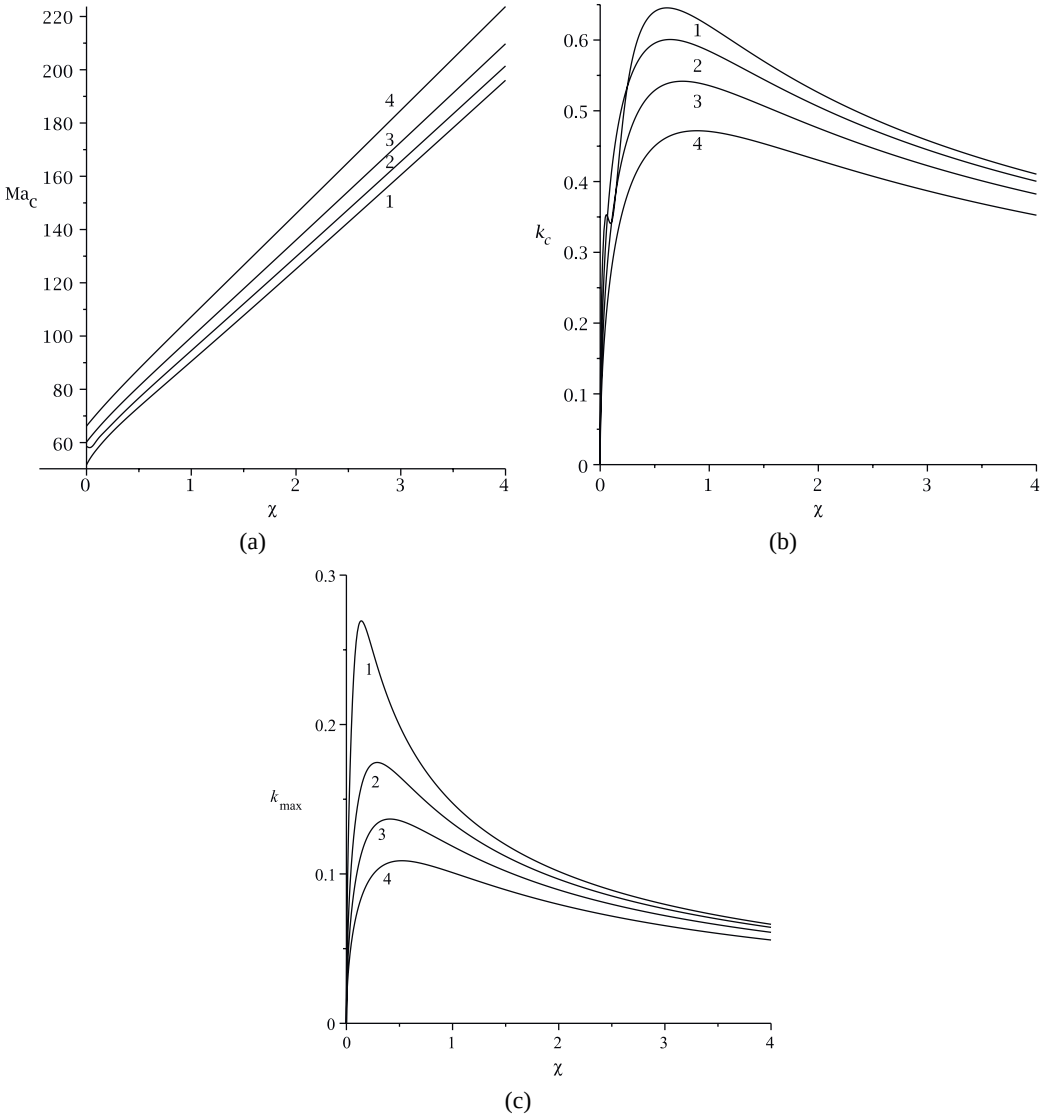

FIG. 5: bi = 0.1, d_W = 1; (a) Ma_C vs χ; (b) k_C vs χ; and (c) most dangerous mode $k_{\max}$ vs χ (for $\varepsilon^4 \mathrm{Ma}_{2S} = 0.1$); d = (1) 0.1, (2) 0.2, (3) 0.3, (4) 0.4

of χ. Notice the peculiar behavior of the curve corresponding to d = 0.1. It is interesting in Fig. 5(c) that the curves of $k_{\max}$ have maxima, too, with respect to χ, as occurs with k_C, but at different magnitudes of χ.

When the relative thickness of fluid 1 d is larger than 1, the Marangoni number is negative as shown in Fig. 6. In Fig. 6(a) for Ma_C it is observed that χ also has a stabilizing effect. It is more stabilizing for d = 1.5. In other words, the stability is enhanced decreasing the relative thickness of fluid 1 when χ increases. The graphs of the critical wave number are presented in two parts due to the peculiar behavior of the curves. In Fig. 6(b) only the range $0 < \chi < 0.05$ is presented to understand how the curve of d = 3 crosses that of d = 4. Figure 6(c) shows how for larger χ the curve of d = 2 crosses those of d = 4 and d = 3 to become the larger critical wave number in a wide range of χ. Each curve shows a maximum which corresponds to the smallest cell size. The wave number corresponding to the maximum growth rate is plotted in Fig. 6(d). Each curve shows one maximum but, in contrast to the curves of k_C in Fig. 6(c), the curves do not intersect each other.

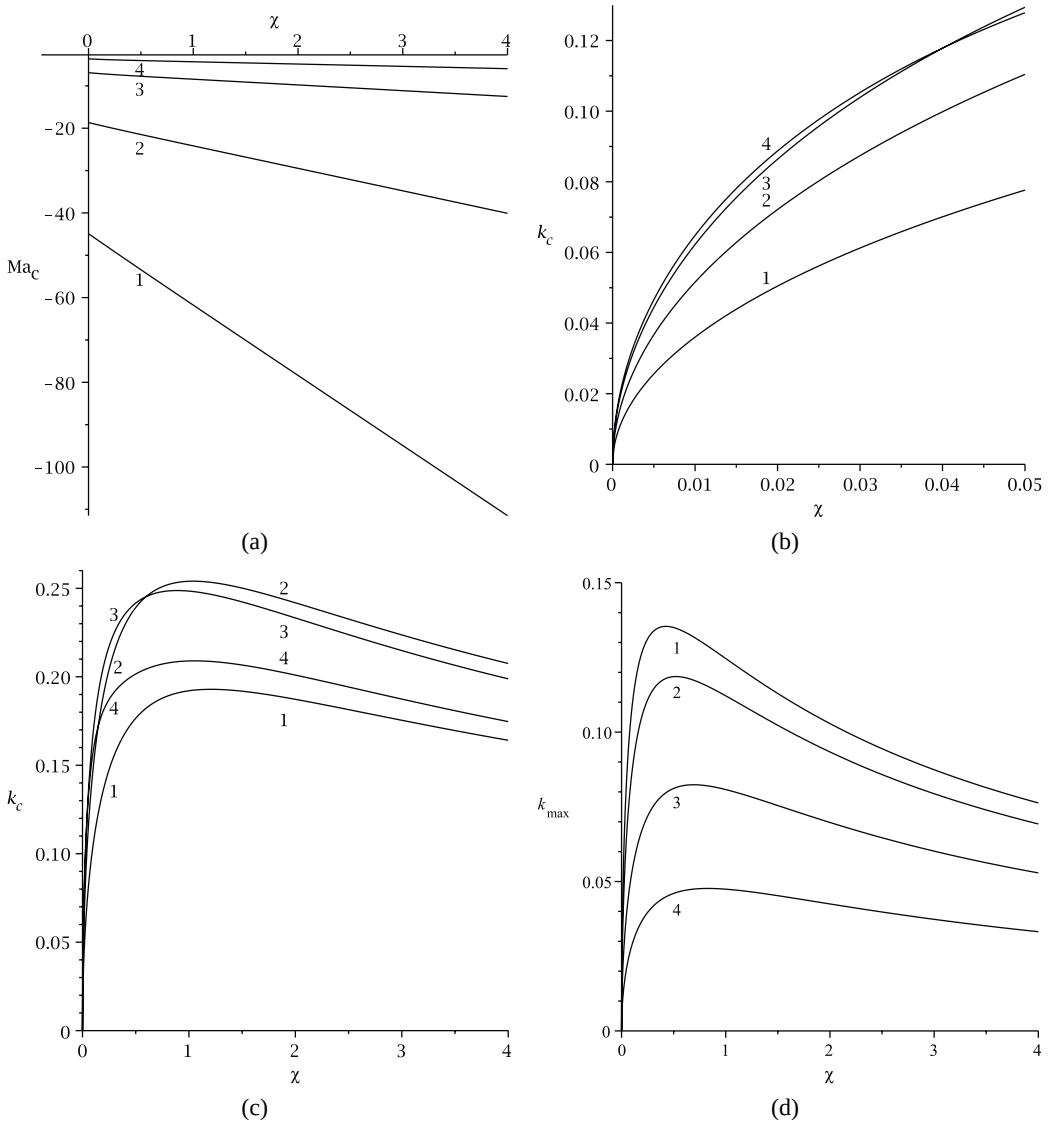

FIG. 6: bi = 0.1, d_W = 1; negative Ma_C; (a) Ma_C vs χ; (b) k_C vs χ, $0 < \chi < 0.05$; (c) k_C vs χ, $0 < \chi < 4$; and (d) most dangerous mode $k_{\max}$ vs d_W (for $\varepsilon^4 \mathrm{Ma}_{2S} = -0.1$); d = (1) 1.5, (2) 2, (3) 3, (4) 4

Figure 7 presents the variation of Ma_C and k_C against the relative thickness of the wall d_W for bi = 0.1 and χ = 0.1. In Fig. 7(a) clearly, the behavior of Ma_C is not monotonous for $d_W \leq 1$. It is destabilizing in some places of the range showing a minimum in each curve. For larger d_W the growth of Ma_C is monotonous. Notice that the increase of d, the relative thickness of fluid 1 is stabilizing. The corresponding graphs of k_C are shown in Fig. 7(b). Here, each curve presents a maximum and has a fast decrease to zero when d_W is finite but very small. Observe that in the picture the curves do not reach the horizontal axis, but in fact they should go directly to a zero critical wave number. The graphs of $k_{\max}$ are given in Fig. 7(c). There, the dashed curves correspond to the region where k_C = 0 and the solid ones correspond to the region where $k_C > 0$. Notice that the solid curve 4 for d = 0.4 nearly touches the vertical axis.

The results for $d > 1$ are presented in Fig. 8 for negative Ma_C. The thickness of fluid 1 is larger than that of fluid 2. As can be seen, the increase of d_W has a stabilizing effect which is enhanced by the decrease of d. As shown, Ma_C

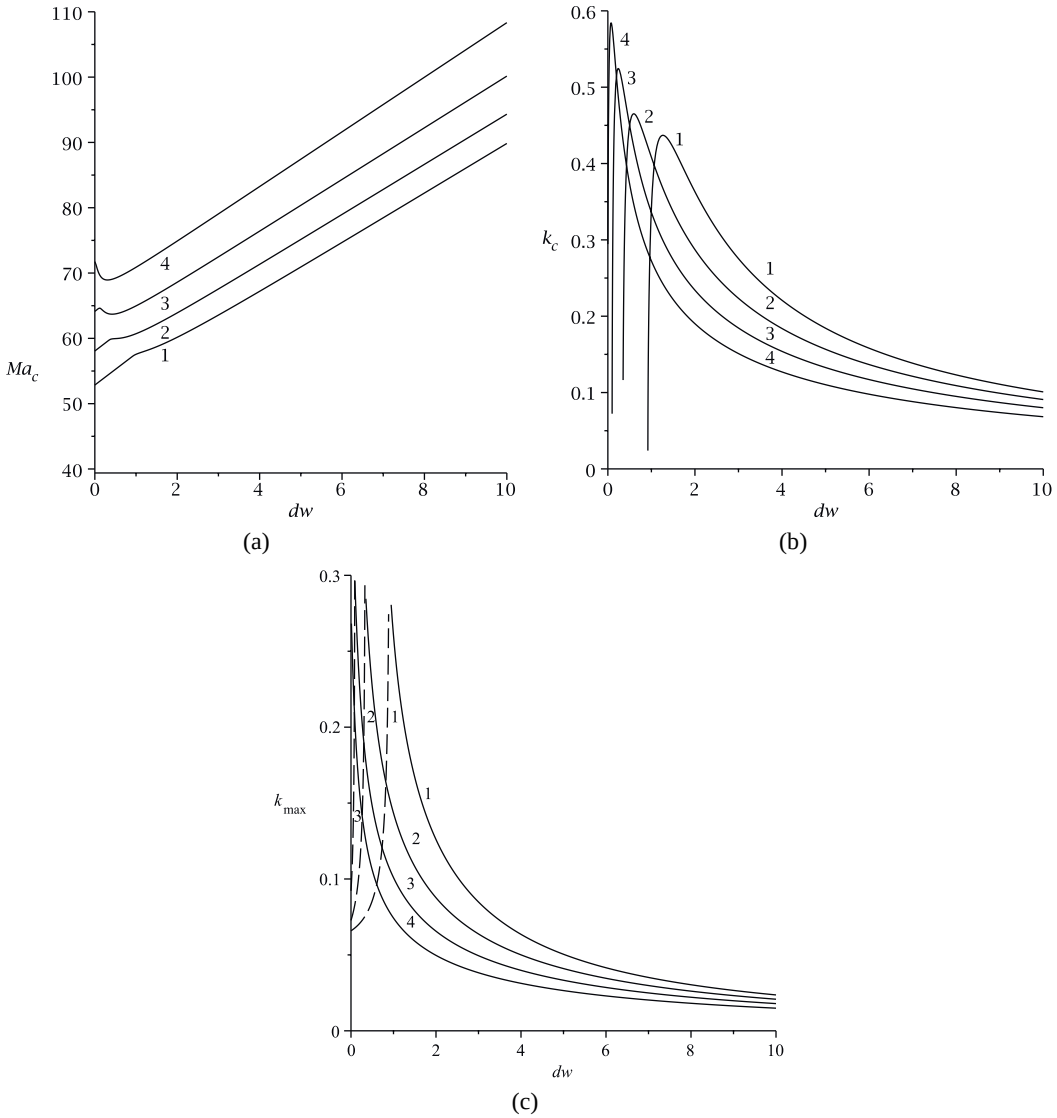

FIG. 7: bi = 0.1, χ = 0.1; (a) Ma_C vs d_W; (b) k_C vs d_W; and (c) most dangerous mode $k_{\max}$ vs d_W, solid when $k_C > 0$ (for $\varepsilon^4\mathrm{Ma}_{2S}$ = 0.1) and dashed when k_C = 0 (for $\varepsilon^2\mathrm{Ma}_{1S}$ = 0.1); d = (1) 0.1, (2) 0.2, (3) 0.3, (4) 0.4

has a very small variation for d = 3 and d = 4, in contrast to curves d = 1.5 and d = 2. In Fig. 8(b) for k_C it is notable that the curves cross each other. Besides, that of d = 4 becomes the larger one when d_W increases. Physically, the convection cells of the smallest size correspond to this. All the curves touch the vertical axis even though the curve of d = 4 presents a maximum. Consequently, k_C has a finite value when d_W = 0. Plots of $k_{\max}$ vs d_W are given in Fig. 8(c). Observe that all the curves have a finite value at d_W = 0 where each one has a maximum and that they show a monotonic decrease with d_W.

4. CONCLUSIONS

The thermocapillary stability of two fluid layers coating both sides of a thick wall with finite thermal conductivity has been investigated. It is assumed that the free surface of each fluid is flat as done by Pearson (1958). Due to the large number of parameters it is supposed that the two liquid layers are made of the same fluid and that their

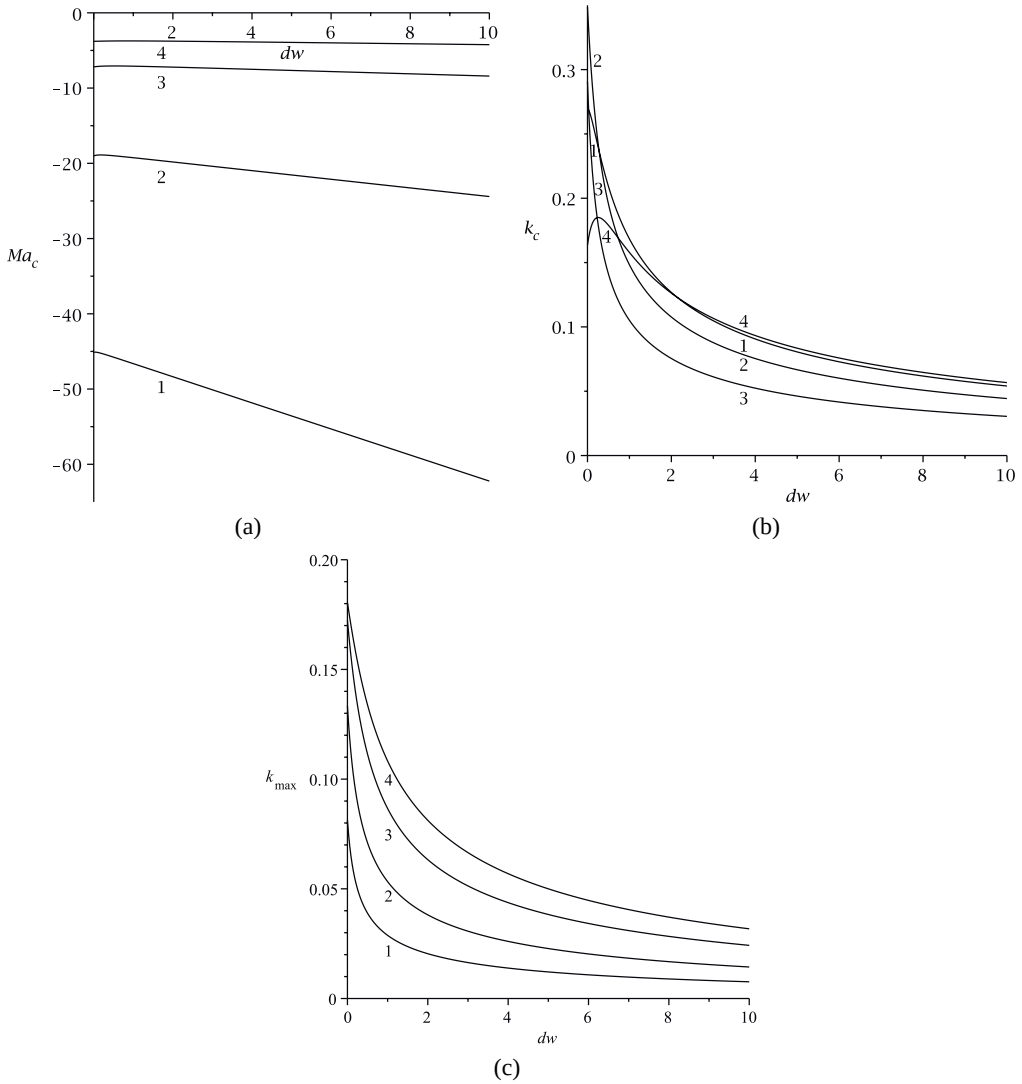

FIG. 8: bi = 0.1, χ = 0.1; negative Ma_C; (a) Ma_C vs d_W; (b) k_C vs d_W; and (c) most dangerous mode $k_{\max}$ vs d_W (for $\varepsilon^4 \mathrm{Ma}_{2S} = -0.1$); d = (1) 1.5, (2) 2, (3) 3, (4) 4

corresponding atmospheres are also the same but at different temperatures. This reduces the number of parameters to a few. Nevertheless, a large variety of phenomena are found. Two possibilities of instability are found. One for a positive critical Marangoni number and another one for a negative one. The negative Ma_C means that now the instability is possible when the atmosphere next to fluid 1 is colder than that next to fluid 2. The former is possible when the relative thickness d of fluid 1 is $d < 1$. The latter corresponds to $d > 1$. The interaction of the two fluids' instabilities leads to interesting results. It is found that for $d < 1$ an increase of the Biot number of fluid 2, bi, gives the possibility of having k_C = 0 after a definite magnitude influenced by d. After this magnitude of bi, Ma_C remains constant because the term Ma_0 in Eq. (29) is independent of bi. However, analytical conditions have been calculated that lead to k_C = 0 when bi is small in a formula obtained asymptotically for small d and d_W = 1. It is interesting that these conditions make this possible even when χ is small but different from zero. The result may be due to the important influence of the finite relative thickness of the wall, d_W, as shown in other problems published in previous papers (Hernández-Hernández and Dávalos-Orozco, 2015; Dávalos-Orozco, 2012, 2014, 2015, 2016).

When the magnitude of k_C is zero and different from zero the curves of $k_{\max}$ have to be calculated by two different formulas, Eqs. (36) and (37), respectively. Each equation has a singularity at the bi where k_C drops to zero. When $d > 1$, Ma_C is negative and $k_{\max}$ increases monotonically.

The variation of χ, the relative wall thermal conductivity, has a stabilizing effect. However, for small magnitudes of χ and particular values of d, the behavior of Ma_C is not monotonic and shows a small depression (more instability). The graphs of k_C present a maximum for every magnitude of d, but it tends to zero when χ tends to zero. If $d >$ 1 the growth of the magnitude of the negative Ma_C is monotonic with χ. However, the growth of k_C is interesting because the curves cross each other increasing χ and the curve that attains the larger critical wave number is that of d = 2, located in the middle range of d investigated. It is noteworthy that the curves of $k_{\max}$ have a maximum for both positive and negative Ma_C.

The relative thickness of the wall also has an interesting effect on Ma_C which here, too, has a small depression (destabilizing effect) when $0 < d_W < 2$. For larger values of d_W the system is stabilized monotonically. The critical wave number also has a maximum for each magnitude of d, but now k_C drops to zero for small enough magnitudes of d_W. When $d > 1$, k_C has maximum only for some magnitudes of d, but, in contrast, k_C has a finite value when d_W = 0. In this case, too, $k_{\max}$ has to be calculated with Eq. (36) when k_C = 0 and with Eq. (37) when $k_C > 0$. However, for $\mathrm{Ma}_C < 0$, $k_{\max}$ has a monotonic decrease with d_W.

In this paper, the complexity of this particular two-fluid system has been reviewed in the form of graphs where a variety of parameters has been used to understand the thermocapillary instability. The effect of the free-surface deformation contributes with another degree of freedom to the instability. The details of the problem have been investigated and are now in preparation for publication.

ACKNOWLEDGMENTS

The author would like to thank Alberto López, Alejandro Pompa, Cain González, Raúl Reyes, Ma. Teresa Vázquez, and Oralia Jiménez for technical support.

REFERENCES

Al-Sibai, F., Leefken, A., and Renz, U., Local and instantaneous distribution of heat transfer rates through wavy films, *Int. J. Therm. Sci.*, vol. **41**, no. 7, pp. 658–663, 2002. DOI: 10.1016/S1290-0729(02)01360-1

Bau, H.H., Control of Marangoni-Bénard convection, *Int. J. Heat Mass Trans.*, vol. **42**, no. 7, pp. 1327–1341, 1999. DOI: 10.1016/S0017-9310(98)00234-8

Catton, I. and Lienhard, V.J.H., Thermal stability two fluid layers separated by a solid interlayer of finite thickness and thermal conductivity, *J. Heat Trans.*, vol. **106**, no. 8, pp. 605–612, 1984. DOI: 10.1115/1.3246722

Chapman, C.J. and Proctor, M.R.E., Nonlinear Rayleigh-Bénard convection between poorly conducting boundaries, *J. Fluid Mech.*, vol. **101**, no. 4, pp. 759–782, 1980. DOI: 10.1017/S0022112080001917

Char, M.-I. and Chen, C.-C., Influence of viscosity variation on the stationary Bénard-Marangoni instability with a boundary slab of finite conductivity, *Acta Mech.*, vol. **135**, no. 3, pp. 181–198, 1999. DOI: 10.1007/BF01305751

Dávalos-Orozco, L.A., Magnetoconvection in a rotating fluid between walls of very low thermal conductivity, *J. Phys. Soc. Jpn.*, vol. **53**, no. 7, pp. 2173–2176, 1984. DOI: 10.1143/JPSJ.53.2173

Dávalos-Orozco, L.A. and Manero, O., Thermoconvective instability of a second-order fluid, *J. Phys. Soc. Jpn.*, vol. **55**, no. 2, pp. 442–445, 1986. DOI: 10.1143/JPSJ.55.442

Dávalos-Orozco, L.A., Thermocapillar instability of liquid sheets in motion, *Colloids Surf. A*, vol. **157**, no. 1, pp. 223–233, 1999. DOI: 10.1016/S0927-7757(99)00093-X

Dávalos-Orozco, L.A., Thermal marangoni convection of a fluid film coating a deformable membrane, *J. Colloid Interface Sci.*, vol. **234**, no. 1, pp. 106–116, 2001. DOI: 10.1006/jcis.2000.7301

Dávalos-Orozco, L.A., The effect of the thermal conductivity and thickness of the wall on the nonlinear instability of a thin film flowing down an incline, *Int. J. Nonlinear Mech.*, vol. **47**, no. 4, pp. 1–7, 2012. DOI: 10.1016/j.ijnonlinmec.2012.02.008

Dávalos-Orozco, L.A., Nonlinear instability of a thin film flowing down a smoothly deformed thick wall of finite thermal conductivity, *Interfac. Phenom. Heat Trans.*, vol. **2**, no. 1, pp. 55–74, 2014. DOI: 10.1615/InterfacPhenomHeatTransfer.2014010400

Dávalos-Orozco, L.A., Non-linear instability of a thin film flowing down a cooled wavy thick wall of finite thermal conductivity, *Phys. Lett. A*, vol. **379**, nos. 12-13, pp. 962–967, 2015. DOI: 10.1016/j.physleta.2015.01.018

Dávalos-Orozco, L.A., Thermal Marangoni instability of a thin film flowing down a thick wall deformed in the backside, *Phys. Fluids*, vol. **28**, no. 5, 054103, 2016. DOI: doi.org/10.1063/1.4948253

Dávalos-Orozco, L.A. and You, X.-Y., Three-dimensional instability of a liquid layer flowing down a heated vertical cylinder, *Phys. Fluids*, vol. **12**, no. 9, pp. 2198–2209, 2000. DOI: 10.1063/1.1286594

Fu, Q.-F., Yang, L.-J., Tong, M.-X., and Wang, C., Absolute and convective instability of a liquid sheet with transverse temperature gradient, *Int. J. Heat Fluid Flow*, vol. **44**, pp. 652–661, 2013. DOI: 10.1016/j.ijheatfluidflow.2013.09.006

Gangadharaiah, Y.H., Onset of surface tension driven convection in a fluid layer with a boundary slab of finite conductivity and deformable free surface, *Int. J. Math Arch.*, vol. **4**, no. 5, pp. 311–323, 2013.

Gershuni, G.Z. and Zhukhovitskii, E.M., Convective instability of a two-layer system with thermally insulated boundaries, *Fluid Dyn.*, vol. **21**, no. 2, pp. 185–190, 1986. DOI: 10.1007/BF01050167

Getachew, D. and Rosenblat, S., Thermocapillary instability of a viscoelastic liquid layer, *Acta Mech.*, vol. **55**, no. 1, pp. 137–149, 1985. DOI: 10.1007/BF01267986

Hernández Hernández, I.J. and Dávalos-Orozco, L.A., Competition between stationary and oscillatory viscoelastic thermocapillary convection of a film coating a thick wall, *Int. J. Therm. Sci.*, vol. **89**, pp. 164–173, 2015. DOI: 10.1016/j.ijthermalsci.2014.11.003

Hurle, D.T.J., Jakeman, E., and Pick, R.E., On the solution of the Bénard problem with boundaries of finite conductivity, *Proc. R. Soc. London, Ser. A*, vol. **296**, no. 1447, pp. 469–475, 1967. DOI: 10.1098/rspa.1967.0039

Kabova, Yu.O. and Kuznetsov, V.V., Downward flow of a nonisothermal thin liquid film with variable viscosity, *J. Appl. Mech. Tech. Phys.*, vol. **43**, no. 6, pp. 895–901, 2002. DOI: 10.1023/A:1020772706082

Kabova, Yu.O., Alexeev, A., Gambaryan-Roisman, T., and Stephan, P., Marangoni-induced deformation and rupture of a liquid film on a heated microstructured wall, *Phys. Fluids*, vol. **18**, no. 012104, pp. 1–15, 2006. DOI: 10.1063/1.2166642

Kalitzova-Kurteva, P.G., Slavtchev, S.G., and Kurtev, I.A., Stationary Marangoni instability in a liquid layer with temperature-dependent viscosity and deformable free surface, *Micrograv. Sci. Technol.*, vol. **9**, no. 4, pp. 257–263, 1996.

Kechil, S.A. and Hashim, I., Oscillatory Marangoni convection in variable viscosity fluid layer: The effect of thermal feedback control, *Int. J. Therm. Sci.*, vol. **48**, no. 6, pp. 1102–1107, 2009. DOI: 10.1016/j.ijthermalsci.2008.11.008

Lienhard, J.H. and Catton, I., Heat transfer across a two-fluid-layer region, *J. Heat Trans.*, vol. **108**, no. 2, pp. 198–205, 1986. DOI: 10.1115/1.3246887

McTaggart, C.L., Convection driven by concentration and temperature dependent surface tension, *J. Fluid Mech.*, vol. **134**, pp. 301–310, 1983. DOI: 10.1017/S0022112083003377

Moctezuma-Sánchez, M. and Dávalos-Orozco, L.A., Azimuthal instability modes in a viscoelastic liquid layer flowing down a heated cylinder, *Int. J. Heat Mass Trans.*, vol. **90**, pp. 15–25, 2015. DOI: 10.1016/j.ijheatmasstransfer.2015.06.035

Nepomnyashchy, A. and Simanovskii, I., Thermocapillary convection in a two-layer system, *Fluid Dyn.*, vol. **18**, no. 4, pp. 629–633, 1983. DOI: 10.1007/BF01090632

Nepomnyashchy, A. and Simanovskii, I., Oscillatory regimes of convection in a two-layer system, *J. Eng. Phys. Thermophys.*,

vol. **46**, no. 5, pp. 619–622, 1984. DOI: 10.1007/BF00828049

Nepomnyashchy, A. and Simanovskii, I., Oscillatory convective instability of the equilibrium of two-layer systems in the presence of thermocapillary effect, *J. Appl. Mech. Tech. Phys.*, vol. **1**, no. 1, pp. 55–57, 1985.

Nepomnyashchy, A. and Simanovskii, I., Thermocapillary convection in two-layer systems in the presence of a surface active agent at the interface, *Fluid Dyn.*, vol. **21**, no. 2, pp. 169–174, 1986. DOI: 10.1007/BF01050164

Nepomnyashchy, A., Simanovskii, I., and Legros, J.C., *Interfacial Convection in Multilayer Systems*, 2nd Edition, New York, NY: Springer, 2012.

Or, A.C., Kelly, R.E., Cortelezzi, L., and Speyer, J.L., Control of long-wavelength Marangoni-Bénard convection, *J. Fluid Mech.*, vol. **387**, pp. 321–341, 1999. DOI: 10.1017/S0022112099004607

Oron, A., Deissler, R.J., and Duh, J.C., Marangoni instability in a liquid sheet, *Adv. Space Res.*, vol. **16**, no. 7, pp. 83–86, 1995a. DOI: 10.1016/0273-1177(95)00139-6

Oron, A., Deissler, R.J., and Duh, J.C., Marangoni instability in a liquid layer with two free surfaces, *Eur. J. Mech. B/Fluids*, vol. **14**, no. 6, pp. 737–760, 1995b. DOI: 0273-l 177(95)00139

Pearson, J.R.A., On convection cells induced by surface tension, *J. Fluid Mech.*, vol. **4**, no. 5, pp. 482–500, 1958. DOI: 10.1017/S0022112058000616

Pérez-Reyes, I. and Dávalos-Orozco, L.A., Vorticity effects in the non-linear long wavelength convective instability of a viscoelastic fluid layer, *J. Non-Newtonian Fluid Mech.*, vols. **208–209**, pp. 18–26, 2014. DOI: 10.1016/j.jnnfm.2014.03.009

Proctor, M.R.E., Planform selection by finite-amplitude thermal convection between poorly conducting slabs, *J. Fluid Mech.*, vol. **113**, pp. 469–485, 1981. DOI: 10.1017/S0022112081003595

Scriven, L.E. and Sternling, C.V., On cellular convection driven by surface-tension gradients: Effects of means surface tension and surface viscosity, *J. Fluid Mech.*, vol. **19**, no. 3, pp. 321–340, 1964. DOI: 10.1017/S0022112064000751

Slavtchev, S. and Ouzounov, V., Stationary Marangoni instability in a liquid layer with temperature-dependent viscosity in microgravity, *Micrograv. Q.*, vol. **4**, no. 1, pp. 33–38, 1994.

Slavtchev, S.G., Kalitzova-Kurteva, P.G., and Kurtev, I.A., Oscillatory Marangoni instability in a liquid layer with temperature-dependent viscosity and deformable free surface, *Micrograv. Sci. Technol.*, vol. **11**, no. 1, pp. 29–34, 1998.

Takashima, M., Surface-tension driven convection with boundary slab of finite conductivity, *J. Phys. Soc. Jpn.*, vol. **29**, no. 2, p. 531, 1970. DOI: 10.1143/JPSJ.29.531

Takashima, M., Surface tension driven instability in a horizontal liquid layer with a deformable free surface. I. Stationary convection, *J. Phys. Soc. Jpn.* **50**, no. 8, pp. 2745–2750, 1981a. DOI: 10.1143/JPSJ.50.2745

Takashima, M., Surface tension driven instability in a horizontal liquid layer with a deformable free surface. II. Overstability, *J. Phys. Soc. Jpn.*, vol. **50**, no. 8, pp. 2751–2756, 1981b. DOI: 10.1143/JPSJ.50.2751

Tong, M.-X., Yang, L.-J., and Fu, Q.-F., Thermocapillar instability of a two-dimensional viscoelastic planar liquid sheet in surrounding gas, *Phys. Fluids*, vol. **26**, no. 3, 033105, 2014. DOI: 10.1063/1.4869716

Yang, H.Q., Boundary effect on the Bénard-Marangoni instability, *Int. J. Heat Mass Trans.*, vol. **35**, no. 10, pp. 2413–2420, 1992. DOI: 10.1016/0017-9310(92)90083-5

APPENDIX

This Appendix presents the equations of motion and heat transfer at the different orders used in this paper along with their corresponding boundary conditions. At zeroth order for fluid 2, they are

$$\frac{d^4 W_0}{dz^4} = 0, \tag{A.1}$$

$$\text{with} \quad W_0 = 0 \quad \text{at} \quad z = 0 \quad \text{and} \quad W_0 = 0, \quad \frac{d^2 W_0}{dz^2} + k_S^2 \mathrm{Ma}_0 \tau_0 = 0 \quad \text{at} \quad z = 1, \tag{A.2}$$

$$\frac{d^2 \tau_0}{dz^2} = 0, \tag{A.3}$$

$$\text{with} \quad \tau_0 = \tau_{W0}, \quad \frac{d\tau_0}{dz} = \chi \frac{d\tau_{W0}}{dz} \quad \text{at} \quad z = 0, \quad \text{and} \quad \frac{d\tau_0}{dz} = 0, \quad \text{at} \quad z = 1. \tag{A.4}$$

At zeroth order for fluid 1, they are

$$\frac{d^4 W_{10}}{dz^4} = 0, \tag{A.5}$$

$$\text{with} \quad W_{10} = 0 \quad \text{at} \quad z = -d_W \quad \text{and} \quad W_{10} = 0, \quad \frac{d^2 W_{10}}{dz^2} - \gamma_T k_S^2 \text{Ma}_0 \tau_{10} = 0 \quad \text{at} \quad z = -d_W - d, \tag{A.6}$$

$$\frac{d^2 \tau_{10}}{dz^2} = 0, \tag{A.7}$$

$$\text{with} \quad \tau_{10} = \tau_{W0}, \quad \frac{d\tau_{10}}{dz} = \frac{\chi}{K} \frac{d\tau_{W0}}{dz} \quad \text{at} \quad z = -d_W, \quad \text{and} \quad \frac{d\tau_{10}}{dz} = 0, \quad \text{at} \quad z = -d_W - d. \tag{A.8}$$

At zeroth order for the wall, it is:

$$\frac{d^2 \tau_{W0}}{dz^2} = 0, \tag{A.9}$$

which needs the boundary conditions presented above. At this order the solution of the three temperatures are equal and are normalized to 1. That is, $\tau_0 = \tau_{W0} = \tau_{10} = 1$. A solvability condition is obtained from Eqs. (A.12), (A.17), and (A.19) of the temperatures at the next order using the boundary conditions. It consists of a system of two homogeneous algebraic equations from which it is possible to obtain Ma_0. One of the constants remains undetermined but simplifies automatically in the process.

Now the equations at the next order are presented. At first order for fluid 2, they are

$$\frac{d^4 W_1}{dz^4} - 2k_S^2 \frac{d^2 W_0}{dz^2} = 0, \tag{A.10}$$

$$\text{with} \quad W_1 = 0 \quad \text{at} \quad z = 0 \quad \text{and} \quad W_1 = 0, \quad \frac{d^2 W_1}{dz^2} + k_S^2 \left(\text{Ma}_0 \tau_1 + \text{Ma}_{1S} \tau_0\right) = 0 \quad \text{at} \quad z = 1, \tag{A.11}$$

$$\frac{d^2 \tau_1}{dz^2} - k_S^2 \tau_0 + W_0 = 0, \tag{A.12}$$

$$\text{with} \quad \tau_1 = \tau_{W1}, \quad \frac{d\tau_1}{dz} = \chi \frac{d\tau_{W1}}{dz} \quad \text{at} \quad z = 0 \quad \text{and} \quad \frac{d\tau_1}{dz} = 0, \quad \text{at} \quad z = 1. \tag{A.13}$$

At first order for fluid 1, they are

$$\frac{d^4 W_{11}}{dz^4} - 2k_S^2 \frac{d^2 W_{10}}{dz^2} = 0, \tag{A.14}$$

$$\text{with} \quad W_{11} = 0 \quad \text{at} \quad z = -d_W, \tag{A.15}$$

$$\text{and with} \quad W_{11} = 0, \quad \frac{d^2 W_{11}}{dz^2} - \gamma_T k_S^2 \left(\text{Ma}_0 \tau_{11} - \gamma_T \text{Ma}_{1S} \tau_{10}\right) = 0 \quad \text{at} \quad z = -d_W - d, \tag{A.16}$$

$$\alpha \left(\frac{d^2 \tau_{11}}{dz^2} - k_S^2 \tau_{10} \right) + \frac{W_{10}}{K} = 0, \tag{A.17}$$

$$\text{with} \quad \tau_{11} = \tau_{W1}, \quad \frac{d\tau_{11}}{dz} = \frac{\chi}{K} \frac{d\tau_{W1}}{dz} \quad \text{at} \quad z = -d_W, \quad \text{and} \quad \frac{d\tau_{11}}{dz} = 0, \quad \text{at} \quad z = -d_W - d. \tag{A.18}$$

At first order for the wall, it is

$$\frac{d^2 \tau_{W1}}{dz^2} - k_S^2 \tau_{W0} = 0. \tag{A.19}$$

Here, too, a solvability condition of two homogeneous algebraic equations is obtained from Eqs. (A.23), (A.28), and (A.31) of the temperatures in the next order using their corresponding boundary conditions. From them it is possible to calculate σ_0, the lowest-order growth rate. A constant remains undetermined but it simplifies after substitution of Ma_0. Consequently, Ma_{1S} is obtained in the marginal state when $\sigma_0 = 0$.

The equations at the next order are the following. At second order for fluid 2, they are

$$\frac{d^4W_2}{dz^4} - 2k_S^2\frac{d^2W_1}{dz^2} + k_S^4W_0 - \frac{\sigma_0}{\mathrm{Pr}}\frac{d^2W_0}{dz^2} = 0, \tag{A.20}$$

$$\text{with} \quad W_2 = 0 \quad \text{at} \quad z = 0, \tag{A.21}$$

$$\text{and with} \quad W_2 = 0, \quad \frac{d^2W_2}{dz^2} + k_S^2\left(\mathrm{Ma}_0\tau_2 + \mathrm{Ma}_{1S}\tau_1 + \mathrm{Ma}_{2S}\tau_0\right) = 0 \quad \text{at} \quad z = 1, \tag{A.22}$$

$$\frac{d^2\tau_2}{dz^2} - k_S^2\tau_1 + W_1 - \sigma_0\tau_0 = 0, \tag{A.23}$$

$$\text{with} \quad \tau_2 = \tau_{W2}, \quad \frac{d\tau_2}{dz} = \chi\frac{d\tau_{W2}}{dz} \quad \text{at} \quad z = 0, \quad \text{and} \quad \frac{d\tau_2}{dz} + \mathrm{bi}k_S^4\tau_0 = 0, \quad \text{at} \quad z = 1. \tag{A.24}$$

At second order for fluid 1, they are

$$\frac{\mu}{\rho}\left(\frac{d^4W_{12}}{dz^4} - 2k_S^2\frac{d^2W_{11}}{dz^2} + k_S^4W_{10}\right) - \frac{\sigma_0}{\mathrm{Pr}}\frac{d^2W_{10}}{dz^2} = 0, \tag{A.25}$$

$$\text{with} \quad W_{12} = 0 \quad \text{at} \quad z = -d_W, \tag{A.26}$$

$$\text{and with} \quad W_{12} = 0, \quad \frac{d^2W_{12}}{dz^2} - \gamma_T k_S^2\left(\mathrm{Ma}_0\tau_{12} + \mathrm{Ma}_{1S}\tau_{11} + \mathrm{Ma}_{2S}\tau_{10}\right) = 0 \quad \text{at} \quad z = -d_W - d, \tag{A.27}$$

$$\alpha\left(\frac{d^2\tau_{12}}{dz^2} - k_S^2\tau_{11}\right) + \frac{W_{11}}{K} - \sigma_0\tau_{10} = 0, \tag{A.28}$$

$$\text{with} \quad \tau_{12} = \tau_{W2}, \quad \frac{d\tau_{12}}{dz} = \frac{\chi}{K}\frac{d\tau_{W2}}{dz} \quad \text{at} \quad z = -d_W, \tag{A.29}$$

$$\text{and with} \quad \frac{d\tau_{12}}{dz} - \frac{\mathrm{bi}_1}{d}k_S^4\tau_{10} = 0, \quad \text{at} \quad z = -d_W - d. \tag{A.30}$$

At second order for the wall, it is

$$\left[\chi\Big/\left(\frac{\rho_W}{\rho_2}\frac{cp_W}{cp_2}\right)\right]\left(\frac{d^2\tau_{W2}}{dz^2} - k_S^2\tau_{W1}\right) - \sigma_0\tau_{W0} = 0, \tag{A.31}$$

which uses the above boundary conditions. For the third order only the following Eqs. (A.32), (A.34), and (A.36) of the temperatures are needed along with their boundary conditions.

$$\frac{d^2\tau_3}{dz^2} - k^2\tau_2 + W_2 - \sigma_0\tau_1 - \sigma_1\tau_0 = 0, \tag{A.32}$$

$$\text{with} \quad \tau_3 = \tau_{W3}, \quad \frac{d\tau_3}{dz} = \chi\frac{d\tau_{W3}}{dz} \quad \text{at} \quad z = 0, \quad \text{and} \quad \frac{d\tau_3}{dz} + \mathrm{bi}k^4\tau_1 = 0 \quad \text{at} \quad z = 1, \tag{A.33}$$

$$\alpha\left(\frac{d^2\tau_{13}}{dz^2} - k^2\tau_{12}\right) + \frac{W_{12}}{K} - \sigma_0\tau_{11} - \sigma_1\tau_{10} = 0, \tag{A.34}$$

$$\begin{gathered}\text{with} \quad \tau_{13} = \tau_{W3}, \quad \frac{d\tau_{13}}{dz} = \frac{\chi}{K}\frac{d\tau_{W3}}{dz} \quad \text{at} \quad z = -d_W, \\ \text{and} \quad \frac{d\tau_{13}}{dz} - \frac{\mathrm{bi}_1}{d}k^4\tau_{11} = 0 \quad \text{at} \quad z = -d_W - d,\end{gathered} \tag{A.35}$$

$$\left[\chi\Big/\left(\frac{\rho_W}{\rho_2}\frac{cp_W}{cp_2}\right)\right]\left(\frac{d^2\tau_{W3}}{dz^2} - k^2\tau_{W2}\right) - \sigma_0\tau_{W1} - \sigma_1\tau_{W0} = 0. \tag{A.36}$$

A solvability condition is obtained which is useful to get σ_1 assuming that $\sigma_0 = 0$. One constant remains undetermined but it simplifies in the final expression after substitution of the previous Ma_0 and Ma_{1S}. In the marginal stationary state it is assumed that $\sigma_1 = 0$, the condition from which Ma_{2S} is calculated.